



OPEN

Diagnostic reference level, achievable dose, and effective dose estimation in adult hybrid SPECT myocardial perfusion imaging in Institut Jantung Negara

Haniff Shazwan Safwan Selvam[✉], Ahmad Khairuddin Mohamed Yusof, Muhammad Azuan Nazri, Norizan Omar, Ali Hazizi Jamal Harizan, Norizam Mois & Muhd Zaidi Ab Rahman

This study aims to establish the diagnostic reference level (DRL), achievable dose (AD), and effective dose (ED) estimation for adult hybrid SPECT myocardial perfusion imaging (MPI) procedures at Institut Jantung Negara (IJN). 737 subjects referred for MPI studies from January to June 2024 were included in the analysis. These subjects underwent either a one-day or two-day Tc-99 m tetrofosmin protocol using a cardiac-dedicated single-photon emission computed tomography (SPECT), either GE SPECT Discovery NM530c or GE SPECT Ventri. All subjects also underwent a cardiac CT scan via an external positron emission tomography/computed tomography (PET/CT) system, GE Discovery MI Digital Ready for either CT attenuation correction (CTAC) or CT coronary artery calcium score (CAC) protocol, depending on their clinical condition. The one-day protocol showed AD of 240.50 MBq and 691.90 MBq for the first and second injections, respectively, with corresponding DRL of 263.63 MBq and 777.93 MBq. The two-day protocol involved higher ADs of 1106.30 MBq and 1073.00 MBq for the first and second injections, with DRL of 1239.50 MBq and 1221.00 MBq, respectively. In the CTAC protocol, the AD for CT dose index volume (CTDI_{vol}) was 2.8 mGy, with a DRL of 4.3 mGy. The dose length product (DLP) had an AD of 53.1 mGy.cm, compared to a DRL of 78.6 mGy.cm. For the CAC protocol, the CTDI_{vol} had an AD of 4.8 mGy, matching the DRL of 4.8 mGy. The DLP showed an AD of 67.8 mGy.cm, with a DRL of 77.5 mGy.cm. The mean cumulated effective dose ($\text{ED}_{\text{CUMULATED}}$) for one-day/CTAC, one-day/CAC, two-day/CTAC, and two-day/CAC was 6.69 ± 1.76 mSv, 7.32 ± 1.37 mSv, 10.13 ± 5.31 mSv, and 13.99 ± 3.24 mSv respectively. The average ED relative contribution by SPECT and CT were found to be 78.3% and 21.7% respectively. The DRL, AD, and ED data were successfully established for local MPI practice, contributing to global efforts to harmonize and enhance radiation safety in MPI practices.

Keywords DRL, AD, AD, MPI, SPECT, Effective dose, Radiation safety

Coronary artery disease (CAD), a leading cause of cardiovascular mortality in the world, is a disorder that occurs due to atherosclerotic occlusions of the coronary arteries. It is manifested by stable or unstable angina, myocardial infarction, sudden cardiac death and/or heart failure^{1,2}. Single photon emission computed tomography (SPECT) myocardial perfusion imaging (MPI) is a well-established non-invasive diagnostic method to diagnose myocardial ischemia or infarctions in patients with known or suspected CAD³. SPECT MPI provides valuable information about the severity and extension of CAD, which helps in patient management⁴⁻⁶. With the advancement and the introduction of semi-conductor detector, cadmium zinc telluride (CZT) SPECT, the advantages are in the reduction of radiation doses, shorter acquisition time and improved overall detection efficiency⁷.

Technetium-99 m (Tc-99 m) is a gamma-emitting radioisotope with a principal photon energy of 140 keV and a physical half-life of 6.04 h. Tetrofosmin (Myoview™) is a pharmaceutical agent that is a lipophilic cationic diphosphine (trans-dioxo-bis) complex. When Tc-99 m pertechnetate (unlabelled Tc-99 m) is added

Imaging Centre, Institut Jantung Negara, No 145 Jalan Tun Razak, 50400 Kuala Lumpur, Malaysia. [✉]email: anepshazwan@gmail.com

to tetrofosmin in the presence of the reducing agent stannous ion, a lipophilic, cationic Tc-99 m tetrofosmin complex is formed⁸. Tc-99 m tetrofosmin is a cationic diphosphine with good myocardial uptake (first-pass extraction efficiency of ~ 50%) and retention with little redistribution from the myocardium over time⁹. Alternatively, radiotracers such as technetium-99 m radiolabelled with sestamibi or thallium-201 could be the other options for this study¹⁰.

The computed tomography (CT) coronary artery calcium score (CAC) is a non-invasive assessment used to evaluate the amount of coronary atherosclerosis. CAC can be used alone or alongside MPI, offering detailed anatomical insights into coronary health alongside MPI's functional information. It helps further with risk stratification, assist in the assessment and guides management of patients with known or suspected CAD¹¹. Integrating a CAC score with MPI provides complementary information in the form of coronary anatomical assessment alongside the presence or absence of ischemia^{12,13}. The use of CAC is beneficial for assessing coronary artery disease risk, adding more critical information in MPI's findings. However, it is crucial to consider the cumulative radiation dose to the patient when incorporating CAC into routine clinical practice.

Diagnostic reference level (DRL) and achievable dose (AD) are critical tools in medical imaging for ensuring patient radiation safety^{14,15}. The DRL is defined as the 75th percentile of radiation exposure in regional or national surveys. DRL is used to identify situations where the doses may be unusually high. AD, representing the median or 50th percentile, is a newer standard aimed at representing doses realistically achievable by centres that are using standard techniques and commonly available equipment^{14,16}. These benchmarks help imaging facilities evaluate and potentially adjust their protocols to optimize patient safety, with DRL acting as an upper threshold for review, and AD offering a broader target for routine practices. This study aims to establish a local baseline for DRL and AD in SPECT MPI at a single centre, thereby addressing the gaps in Malaysia's current national DRL (NDRL), which was based on limited institutional data from 2005 to 2007. By analysing data within a single centre, this study aims to compare results with other studies to improve radiation safety and optimize local imaging practices. Moreover, establishing a locally relevant baseline can serve as a model for nationwide and international adoption of SPECT MPI procedures, contributing to the ongoing improvements in radiation protocols and providing valuable data for refining future NDRL and other international standards.

Methods

Study design

This study was approved by IJN Research Ethics Committee (project registration ID IJNREC/651/2024). It was a six-month retrospective study conducted from January 2024 to June 2024 by reviewing image data of adult patients referred for MPI study to this institution. Informed consent for each recorded data was waived by IJN Research Ethics Committee prior to study initiation. No major protocol changes occurred during the study period. Patients had MPI scan (either one-day or two-day protocol) using a cardiac-dedicated gamma cameras, followed by an external computed tomography (CT) scan for CT attenuation correction (CTAC) or CT coronary artery calcium score (CAC) using our multi-slice CT modality in positron emission tomography/computed tomography (PET/CT). The inclusion criteria for this study comprised patients aged 18 years and older, those referred for MPI between January 2024 and June 2024, and patients with available and complete imaging data in the database. Exclusion criteria included patients aged 17 years and younger, those with missing or incomplete imaging records, patients who experienced protocol deviations that did not align with the routine MPI workflow during the study period, and those whose scans had technical failures such as corrupted imaging files, acquisition errors, or unacceptable image quality as determined by physicians.

Myocardial perfusion imaging (MPI) protocol

The MPI protocol was adapted from American Society of Nuclear Cardiology (ASNC) guideline¹⁷. It includes the indications, contraindications, patient preparation, selection and dosage of stressing agents as well as SPECT imaging schedule for conducting MPI studies.

SPECT modalities

A cardiac-dedicated CZT gamma camera (Discovery NM 530c; GE Healthcare, Milwaukee, WI, USA) and cardiac-dedicated conventional gamma camera (Vetri; GE Healthcare, Milwaukee, WI, USA) were used to collect SPECT data, designated as GC-1 and GC-2, respectively. The CT modality was not available on both systems; hence, the CT portion was acquired using a PET/CT scanner (GE Discovery MI Digital Ready; GE Healthcare, Milwaukee, WI, USA) that incorporated with 128-CT slices system. Table 1 shows the general properties of SPECT modalities incorporated in our MPI practice.

Activity prescription technique

All patients received Tc-99 m tetrofosmin (Myoview; GE Healthcare, USA), with activity prescribed using a weight-based approach. The prescribed activity varied based on the imaging system (GC-1 or GC-2) and the selected MPI protocol, whether a one-day or two-day protocol. Details of protocol selection and activity prescription for both systems are presented in Table 2.

SPECT acquisition

The choice of a one-day or two-day MPI protocol was primarily based on the subject's body mass index (BMI). Patients with a BMI of 35 or higher generally underwent the two-day protocol to minimize radiation exposure, as higher activity were required due to increased body weight. In contrast, those with a BMI of 35 or lower were typically assigned to the one-day protocol. However, in certain cases, additional factors such as patient logistics were also considered when determining the appropriate protocol. Similarly, the choice of imaging system, either GC-1 or GC-2, was also influenced by BMI. Subjects with a BMI under 35 were primarily assigned to GC-

Model	GE discovery NM 530c	GE Venti
Denotation in our study	GC-1	GC-2
Description	Direct conversion, solid-state SPECT detectors	Two externally mounted rectangular detectors.
Diameter of gantry bore	70 cm	70 cm
Crystal detector type	Cadmium Zinc Telluride (CZT)	Sodium Iodide (NaI)
Collimator Type	19 pinhole detectors	Parallel hole collimators - Low energy high resolution
Energy range (keV)	40–200 keV	40–200 keV (depending on collimator type)
Spatial resolution full width half maximum (FWHM) (mm)	Pixel Pitch – 2.46 mm	Useful field of view – 3.7 mm
Energy resolution at 140 keV	5.40%	9.30%
SPECT Tc-99 m point source sensitivity (cps/mCi)	14.93	5.71
Maximum count rate in 20% window (kcps)	≥ 370	≤ 320
SPECT resolution with scatter at 140 keV (mm)	Central – ≤ 6.5 mm	Central – ≤ 10.9 mm
	Tangential – ≤ 4.7 mm	Tangential – ≤ 7.5 mm
	Radial – ≤ 4.7 mm	Radial – ≤ 10.9 mm

Table 1. General specifications of GC-1 and GC-2.

Protocol	BMI	Gamma camera	First injection	Second injection
One-day protocol	BMI ≤ 35	GC-1	2.96 MBq/kg – minimum 148 MBq and maximum 370 MBq	Multiply first dose with factor of 3 – maximum 925 MBq
			≤ 64 kg: 481 MBq (minimum)	Multiply first dose with factor of 2 (maximum: 1100 MBq)
			65–79 kg: 518 MBq	
		GC-2	80–89 kg: 555 MBq	
			90–93 kg: 592 MBq	
			≥ 94 kg: 666 MBq (maximum)	
Two-day protocol	BMI ≥ 35	GC-1	370 MBq	370 MBq
		GC-2	11.47 MBq/kg (Min: Nil, Max: 1480 MBq*)	Same as first dose

Table 2. Activity prescription of Tc-99 m Tetrofosmin for one-day and two-day MPI protocol. *It is recommended to discuss with radiation protection officer (RPO) and physician's opinion to prescribe activity for body weight that resulted more than 1480 MBq.

1, while those with a BMI of 35 or higher were generally assigned to GC-2 to ensure consistency in image quality¹⁸. However, some subjects with a BMI of 35 or higher may have been scanned using GC-1 if they could be accommodated comfortably within the gantry. Table 3 presents the SPECT acquisition protocol for GC-1 and GC-2.

CT acquisition

As previously indicated, PET/CT was used as an external modality for CT image acquisition. Depending on subject's coronary artery disease status, they may have undergone CT attenuation correction (CTAC) alone using CTAC protocol or in conjunction with CT coronary artery calcium score (CAC) using the CAC protocol. The CAC protocol was performed for all of subjects except those who had previous of coronary artery bypass grafts (CABG) surgery or those who had undergone triple-vessel percutaneous coronary intervention (PCI) with stents. Table 4 summarizes the details of both CT acquisition protocols.

SPECT image reconstruction

SPECT image reconstruction parameters were taken from routine protocol. Gated images in GC-1 were reconstructed using the maximum likelihood-expectation maximization (MLEM) method, adapted to the 3D geometry of the CZT camera, with CT attenuation correction. Conversely, gated images from GC-2 were reconstructed using the resolution recovery conventional ordered subset expectation maximization (OSEM) method, also with CT attenuation correction. The choice of reconstruction parameters was based on recommendations from the local application specialist in consensus with reporting physician. Image reconstruction was performed using a dedicated workstation, Xeleris version 4.1 (GE Healthcare, Milwaukee, WI, USA) generating standard axes views (short axis, vertical long axis, horizontal long axis) and polar maps of the left ventricle for clinician's review. Table 5 presents the details on the SPECT image reconstruction protocols.

Data analysis

Subject demographics such as age, sex, height and weight, were recorded from each subject's image files in the Picture Archiving and Communication System (PACS) Synapse version 5.7.200 (Fujifilm Medical Systems, USA). BMI was calculated as weight (kilograms) divided by the square of the height (metre²). For SPECT data collection, the scanner choice and administered activity for both stress and rest phases were recorded. For CT

System	GE NM 530c (GC-1)		GE Ventri (GC-2)	
Collimator	19 Pinhole Collimators		Low Energy High Resolution (LEHR)	
Radionuclide	Tc-99 m		Tc-99 m	
Energy window width	140.5 ± 10% keV		140 ± 10% keV	
Phase	Stress	Rest	Stress	Rest
Protocol	SGATE LD	RGATE LD	SGATE EVOLUTION	RGATE EVOLUTION
Gated	Yes	Yes	Yes	Yes
Position	Supine	Supine	Supine	Supine
Contour	Not Applicable	Not Applicable	Circular	Circular
Acquisition Mode	Static	Static	Step and Shoot, 3 intervals over a 180° arc	Step and Shoot, 3 intervals over a 180° arc
Angle	315° (fixed)	315° (fixed)	45° right anterior oblique to 45° left posterior oblique	45° right anterior oblique to 45° left posterior oblique
Direction	Not Applicable	Not Applicable	Counter-clockwise	Counter-clockwise
Gating parameter	8 frames per cycle	8 frames per cycle	8 frames per cycle	8 frames per cycle
Zoom	1.00	1.00	1.00	1.00
Matrix size	32 × 32	32 × 32	64 × 64	64 × 64
Time per view	5 min	3 min	13 s	10 s
Total view	Not applicable	Not applicable	30 steps, 60 views	30 steps, 60 views
Total acquisition time	5 min	3 min	7 min 7 s	8 min 40 s

Table 3. SPECT acquisition protocol for GC-1 and GC-2.

System	GE discovery MI digital ready with 128 CT slices	
Acquisitions	CTAC	CAC
Mode	Low-Dose, Non-Gated	Prospective-ECG Gated
Scan type	Spiral	Axial (Cine Mode)
Tube voltage	120 kVp	120 kVp
Tube current	30–100 mA	215 mA
Rotation time	0.8 s	0.35 s
Rotation length	Full	Segment
Detector coverage	40 mm	20 mm
Image thickness in recon 1 (Primary Recon)	Helical thickness—5.0 mm	Axial thickness—2.5 mm
	Pitch—0.984	Image per rotation—8 images
	Speed—38.37 mm/rot	Cine between images—0.05 s
Reconstructed image	CT Cardiac and CTAC	CT calcium score, CT Cardiac and CTAC
Reconstructed DFOV	Recon 1—50 cm	Recon 1—25 cm
		Recon 2—50 cm
	Recon 2—41.9 cm	Recon 3—41.9 cm
Reconstructed image slice thickness	Recon 1—CTAC – 5.00 mm	Recon 1—CAC – 2.5 mm
		Recon 2—CTAC – 5.00 mm
	Recon 2—CT Cardiac – 1.25 mm	Recon 3—CT Cardiac – 1.25 mm
Matrix size	512 × 512 mm	
Anatomy region	Carina to apex of the heart	

Table 4. CT acquisition protocol for CTAC and CAC.

data, tube voltage, tube current, scan length, CT dose index volume (CTDI_{vol}) and dose length product (DLP) were noted. Data analysis was conducted using IBM SPSS Statistics (Version 30.0; IBM Corp., Armonk, NY, USA) to calculate mean, standard deviation, 50th percentile, and 75th percentile values for both SPECT and CT data. Additionally, CT parameters such as DLP and CTDI_{vol} were tabulated and presented in terms of minimum, maximum, mean ± standard deviation, 50th percentile and 75th percentile values. As previously described, the DRL was assigned to 75th percentile values, while the AD was attributed to 50th percentile values from the tabulated data for both SPECT and CT portions, respectively.

Effective dose (ED) estimation

The most common parameter to assess the radiation burden across different imaging modalities, scanner and protocol is the effective dose (ED), measured in millisieverts (mSv). ED characterizes whole-body exposure from non-uniform radiation exposure as a weighted average of organ absorbed doses. In this study, the effective dose calculation consists of two distinct estimations. The SPECT scan provides information on internal radiation

Protocol	Parameters	One-day protocol		Two-day protocol
GC-1	Non-attenuation correction (NAC)	Algorithm	MLEM	MLEM
		Iterations	30	30
		Regularization	OSL Green	OSL Green
		Alpha	0.4	0.4
		Beta	0.4	0.4
		Post filter	Butterworth	Butterworth
		Frequency	0.4	0.4
		Order	10	10
	CT Attenuation correction	Not included		
GC-2	Attenuation correction (AC)	Algorithm	MLEM	MLEM
		Iterations	60	60
		Regularization	OSL Green	OSL Green
		Alpha	0.7	0.7
		Beta	0.3	0.5
		Post Filter	Butterworth	Butterworth
		Frequency	0.37	0.37
		Order	7	7
	CT Attenuation correction	Included		
GC-2	GC-2	Post filter	Butterworth	Butterworth
		Frequency	0.52	0.40
		Order	5	10
		Algorithm	OSEM	OSEM
		Iterations	12	2
		Subsets	10	10
		CT Attenuation correction	Included	

Table 5. Image reconstruction protocol in GC-1 and GC-2.

exposure, requiring the computation of internal dosimetry, while CT scan assess external radiation exposure, necessitating the calculation of external beam dosimetry.

Effective dose SPECT (ED_{SPECT})

The ED estimation in SPECT, ED_{SPECT}, was calculated using Eq. 1 based on effective dose conversion coefficient per unit administered activity developed by Anderson. These coefficients, were derived and simulated using ICRP/ICRU biokinetic data, computational voxel reference phantoms, and tissue weighting factors from ICRP publications 103 specifically for Tc-99 m tetrofosmin stress and rest subjects. The corresponding values were 0.00515 mSv/MBq (male, stress), 0.00557 mSv/MBq (male, rest), 0.0062 mSv/MBq (female, stress), 0.00672 mSv/MBq (female, rest), respectively^{19,20}.

$$ED_{SPECT} (mSv) = \text{Activity Administered} \times \frac{\text{Effective Dose Coefficient}}{\text{Unit Administered Activity}} \quad (1)$$

Effective dose CT (ED_{CT})

The simplest method and most commonly used method to estimate the ED for CT scans (ED_{CT}) is by multiplying the dose-length-product (DLP), a CT radiation parameter, by an effective dose conversion coefficient, known as a *k-factor*. The DLP, which is specific to CT, is reported on the scanner console after each acquisition and reflects for both the radiation exposure intensity in milliGray (mGy), and the craniocaudal length irradiated, measured in centimetre (cm). In this study, a cardiac-specific *k-factor* of 0.026 mSv·mGy⁻¹cm⁻¹ as proposed by Trattner et al., was applied to determine the ED_{CT} for both CT attenuation correction (CTAC) protocol and coronary artery calcium score (CAC) protocol, using Eq. 2²¹.

$$ED_{CT} (mSv) = \text{Dose Length Product} \times k - \text{factor} \quad (2)$$

Cumulated effective dose (ED_{CUMULATED})

The cumulated effective dose (ED_{CUMULATED}) associated with the combination of ED_{SPECT} and ED_{CT}, resulting from the hybrid imaging technique used in our MPI protocol was calculated using Eq. 3 in the unit of millisieverts (mSv). Since ED_{CUMULATED} represents the combined dose from both SPECT and CT, the relative percentage contribution from each modality was determined to observe their respective contributions to the total radiation exposure.

$$ED_{CUMULATED} (mSv) = ED_{SPECT} + ED_{CT} \quad (3)$$

Parameters	Protocol				p-value
	One-day protocol		Two-day protocol		
Number of subjects	676		61		
	636 (GC-1)	40 (GC-2)	18 (GC-1)	43 (GC-2)	
Number of S-R (R-S)	582 (94)		58 (3)		0.047 ^a
Number of females (%)	195 (28.8%)		26 (42.6%)		0.025 ^a
Number of males (%)	481 (71.2%)		35 (57.4%)		
Mean Age (years old)	66.0 ± 10.2		62.0 ± 12.4		0.004 ^b
Mean Weight (kg)	70.7 ± 12.2		92.7 ± 16.0		< 0.001 ^b
Mean BMI (kg/m ²)	26.5 ± 3.9		35.6 ± 5.7		< 0.001 ^b

Table 6. Subjects demographics across the one-day and the two-day MPI protocol. a – Chi square test. b – Independent T-test.

MPI protocol	Injection	Administered dose MBq (mCi)					p-value
		Mean ± Std dev	Minimum	Maximum	AD	DRL	
One-day (n = 676)	1st	250.02 ± 90.95 (6.76 ± 2.46)	148.00 (4.00)	721.50 (19.50)	240.50 (6.50)	263.63 (7.13)	< 0.001 ^a
	2nd	696.98 ± 153.26 (18.84 ± 4.14)	444.00 (12.00)	1221.00 (33.00)	691.90 (18.70)	777.93 (21.03)	
Two-day (n = 61)	1st	985.93 ± 359.15 (26.65 ± 9.71)	200.17 (5.41)	1472.60 (39.80)	1106.30 (29.90)	1239.50 (33.50)	
	2nd	942.21 ± 362.11 (25.47 ± 9.79)	185.00 (5.00)	1443.00 (39.00)	1073.00 (29.00)	1221.00 (33.00)	

Table 7. Summary of administered activity for Tc-99 m Tetrofosmin in SPECT. *a – Independent t-test. The unit is displayed for both MBq (SI unit for radioactivity) and mCi.

Results

Demographics

A total of 737 subjects were enrolled in this six-month observational study, with 676 subjects assigned to the one-day protocol and 61 subjects to the two-day protocol, as presented in Table 6. Of those assigned to the one-day protocol, 636 subjects underwent imaging with GC-1, while 40 subjects were scanned with GC-2. Conversely, of the 61 subjects in the two-day protocol, 18 were scanned in GC-1 and 43 using GC-2. The one-day protocol group included 481 male (71.2%) and 195 females (28.8%) with a mean age of 66.0 ± 10.2 years, a mean weight of 70.7 ± 12.2 kg and a mean BMI of 26.5 ± 3.9 kg/m². Meanwhile, the two-day protocol group comprised 35 males (57.4%) and 26 females (42.6%), with mean values of 62.0 ± 12.4 years for age, 92.7 ± 16.0 kg for weight and 35.6 ± 5.7 kg/m² for BMI. These findings clearly indicate that the one-day protocol had a significantly larger sample size than the two-day protocol.

SPECT data

The administered activity between the one-day and two-day protocols was examined without distinguishing between stress-rest or rest-stress sequence, as presented in Table 7. For the one-day protocol, the mean, AD, and DRL for the first injection were 250.02 ± 90.95 MBq, 240.50 MBq, and 263.63 MBq, respectively while for the second injection, these values were 696.98 ± 153.26 MBq, 691.90 MBq, and 777.93 MBq. In contrast, for the two-day protocol, the mean, AD, and DRL for the first injection were 985.93 ± 359.15 MBq, 1106.30 MBq, and 1239.50 MBq, and for the second injection, 942.21 ± 362.11 MBq, 1073.00 MBq, and 1221.00 MBq, respectively. These results indicate that the administered activity in the two-day protocol was higher than in the one-day protocol for both injections ($p < 0.001$).

CT data

The summary of CT result is presented in Table 8. Two distinct CT protocols were utilized; CT attenuation correction (CTAC) and coronary artery calcium score (CAC) with the choice of protocol depending on the subject's condition. Among the 737 subjects, 621 underwent CAC protocol, while the remaining subjects underwent the CTAC protocol. For CTAC protocol, the mean, AD, and DRL for the DLP values were 58.5 ± 30.1 mGy.cm, 53.1 mGy.cm, and 78.6 mGy.cm, respectively. The corresponding values for the CTDI_{vol} were 3.1 ± 1.6 mGy, 2.8 mGy, and 4.3 mGy, respectively. In contrast, for the CAC protocol, the DLP had mean, AD and DRL values of 72.3 ± 10.3 mGy.cm, 67.8 mGy.cm, and 77.5 mGy.cm, respectively, while the CTDI_{vol} values were 4.9 ± 0.2 mGy, 4.8 mGy, and 4.8 mGy, respectively. The mean scan lengths were 156.0 ± 21.0 mm for CTAC and 145.0 ± 21.1 mm for CAC. Overall, the values for CAC protocol were significantly higher across all parameters compared to those for CTAC.

		CTAC (<i>n</i> =116)	CAC (<i>n</i> =621)	<i>p</i> -value
	Sample size	116 (102 in one-day, 14 in two-day)	621 (574 in one-day, 47 in two-day)	
	Scan purpose	Attenuation correction/localisation	Diagnostic/localisation and attenuation correction	
DLP	Mean \pm SD	58.5 \pm 30.1	72.3 \pm 10.3	< 0.001 ^a
	Min	22.1	38.8	
	Max	174.3	126.8	
	AD	53.1	67.8	
	DRL	78.6	77.5	
CTDI _{vol}	Mean \pm SD	3.1 \pm 1.6	4.9 \pm 0.2	< 0.001 ^a
	Min	1.4	4.8	
	Max	7.4	7.0	
	AD	2.8	4.8	
	DRL	4.3	4.8	
Scan Length	Mean	156.0 \pm 21.0	145.4 \pm 21.1	< 0.001 ^a
	Min	99.0	73.0	
	Max	267.0	217.5	

Table 8. Summary of CT dose analysis by protocol. a – Independent t-test.

Comparison with other similar findings

A comparison of both SPECT and CT data was made with findings from other studies. As recommended by International Commission on Radiological Protection (ICRP) Publication 135, the comparison primarily prioritized the 75th percentile, or known as DRL, while the 50th percentile, or known as AD, was used only when the DRL from the referenced study was unavailable¹⁵.

SPECT data

The comparison of SPECT data with other studies is shown in Table 9. It can be observed that the lowest DRL and AD for both the first and second injections in one-day tetrofosmin protocol were recorded in our study compared to similar studies. In contrast, for the two-day protocol, the DRL value of administered activity for both injections were higher than in the listed studies, except for the study by Alkhybari et al., whose findings were reported using AD, in which both of our injection values were lower than theirs²². As previously indicated, the majority of subjects in the two-day protocol were assigned to GC-2, which required a higher prescribed activity, thus leading in greater radiation dose to patients.

CT data

A comparison of CTDI_{vol} and DLP in our MPI practice with similar studies are detailed in Table 10. As mentioned earlier, all CT protocols in the MPI study were performed using our PET/CT. Except for data reported by Abe et al. in PET/CT modality, our DRL for CTDI_{vol} in CTAC was higher than those in the other listed studies²⁵. Since Alkhybari et al. reported their findings using AD, it can be observed that our AD value of CTDI_{vol} is lower than their reported value. A similar pattern was observed for CTDI_{vol} value in the CAC protocol. In contrast, for DLP in CTAC, our DRL value was higher than in all listed studies except for those by Abe et al. and Rinscheid et al.^{25,29}. Again, Since Alkhybari et al. reported their finding using AD, our AD value for DLP is lower than theirs. A similar trend was also observed for DLP in the CAC protocol.

Effective dose (ED) data

Table 11 shows the estimated effective dose (ED) from the MPI procedure incorporating contribution from both CT and SPECT imaging modalities. In the one-day and two-day protocol, the mean ED_{SPECT} were 5.42 \pm 1.33 mSv and 11.10 \pm 3.96 mSv, respectively. The mean ED_{CT} for CTAC was 1.42 \pm 0.78 mSv in the one-day protocol and 2.26 \pm 0.87 mSv in the two-day protocol, respectively. In contrast, the mean ED_{CT} of CAC were 1.87 \pm 0.27 mSv in the one-day protocol and 1.94 \pm 0.31 mSv in the two-day protocol.

Figure 1 illustrates the average ED_{CUMULATED} for each protocol category. The mean ED_{CUMULATED} was 6.69 \pm 1.76 mSv for the one-day/CTAC, 7.32 \pm 1.37 mSv for the one-day/CAC, and 10.13 \pm 5.31 mSv for the two-day/CTAC, and 13.99 \pm 3.24 mSv for the two-day/CAC, respectively. The highest mean ED_{CUMULATED} was observed in the two-day/CAC protocol, while the lowest was observed in the one-day/CTAC protocol.

The relative contribution of ED from SPECT and CT was analysed and is further described in Table 12. On average, SPECT accounted for 78.3% of the total ED, while CT contributed 21.7%. This finding indicates that the administered activity of Tc-99 m tetrofosmin was the primary contributor to the total ED in MPI practice.

Discussion

The mean administered activity in the one-day protocol MPI is lower than the two-day protocol in both injections. In addition to having lower body weight, the majority of subjects in the one-day protocol were scanned using GC-1, a cardiac-dedicated SPECT featuring CZT technology³⁴. This system requires lower administered activity of Tc-99 m tetrofosmin while providing shorter scan time and superior image quality.

Protocol	Administered Activities, MBq (mCi)										Becker [▲] ¹⁴	2015	2016	2017	2018	2019	2020	2021	2022	2023	2024	IJN [▲]	
	Injection	50th	75th	50th	75th	50th	75th	50th	75th	50th													
One – day Tc-99 m Tetrofosmin	1st	240.50 (6.50)	263.63 (7.13)	–	–	452.85 ^S (12.23)	–	–	–	–	555.00 ^S	740.00 ^S	388.00 (10.50)	425.00 (11.50)	–	–	–	–	–	–	–		
	2nd	691.90 (18.70)	777.93 (21.03)	–	–	1155.97 ^R (31.24)	–	–	–	–	925.00 ^R	1111.00 ^R	1147.00 (31.00)	1221.00 (33.00)	–	–	–	–	–	–	–		
Two – day Tc-99 m Tetrofosmin	1st	1106.30 (29.90)	1239.50 (33.50)	–	–	1221.00 ^S (33.00)	–	–	–	–	–	–	1084.00 (29.30)	1214.00 (32.80)	–	–	–	–	–	–	699.00 ^R 850.00 ^S		
	2nd	1073.00 (29.00)	1221.00 (33.00)	–	–	1184.00 ^R (32.00)	–	–	–	–	–	–	1110.00 (30.00)	1199.00 (32.40)	–	–	–	–	–	–	–		
One – day Tc-99 m Sestamibi	1st	–	–	–	–	455.10 ^S (12.30)	–	–	–	–	–	–	388.00 (10.50)	115.00 (425.00)	370.00 ^R	444.00 ^R	–	–	–	–	–	–	–
	2nd	–	–	–	–	1147.00 ^R (31.00)	–	–	–	–	–	–	1169.00 (31.60)	1251.00 (33.80)	1110.00 ^S	1110.00 ^S	–	–	–	–	–	–	–
Two – day Tc-99 m Sestamibi	1st	–	–	–	–	1165.50 ^S (31.50)	–	–	–	–	–	–	1089.00 (29.40)	1165.00 (31.50)	740.00 ^R	814.00 ^R	–	–	–	–	–	–	638.00 ^R 830.00 ^S
	2nd	–	–	–	–	1184.00 ^R (32.00)	–	–	–	–	–	–	1110.00 (30.00)	1184.00 (32.00)	870.00 ^S	925.00 ^S	–	–	–	–	–	–	–
One – day Tetrofosmin + Sestamibi (Combine)	1st	–	–	–	–	350.00 ^R	–	–	–	–	414.10 (11.20)	–	–	–	–	–	–	–	–	–	–		
	2nd	–	–	–	–	1150.00 ^S	–	–	–	–	1184 (32.00)	–	–	–	–	–	–	–	–	–	–		
Two – day Tetrofosmin + Sestamibi (Combine)	1st	–	–	–	–	600.00	–	–	–	–	851.00 (23.00)	–	–	–	–	–	–	–	–	–	–		
	2nd	–	–	–	–	600.00	–	–	–	–	888.00 (24.00)	–	–	–	–	–	–	–	–	–	–		

Table 9. Comparison of MPI practice against other published MPI studies in terms of Tc-99 m administered activities in first and second injection. S – Stress phase. R – Rest phase. [▲] – Stress/rest or rest/stress. [∞] – Rest/stress.

Authors	Years	Protocol	Modality	Purpose	CTDI _{vol} (mGy)		DLP (mGy.cm)	
					50th	75th	50th	75th
IJN	2024	CTAC	PET/CT	AC/AL	2.8	4.3	53.1	78.6
		CAC		AC/AL/Dx	4.8	4.8	67.8	77.5
ARPANSA ²³	2023	CT cardiac	SPECT/CT	-	-	2.10	-	50.00
Alkhybary ²²	2023	CT cardiac	SPECT/ CT	AC	1.03	-	24.33	-
		CT cardiac	PET/CT	AC/AL	7.32	-	207.66	-
Rincheid ²⁹	2022	CT cardiac	SPECT/CT and PET/CT	-	-	3.10	-	81.00
Abe ²⁵	2020	CT cardiac	SPECT CT	AC/Dx	1.60	4.06	45.00	84.10
			PET/CT	Dx	5.50	9.03	209.00	388.90
Bebington ³⁰	2019	CT cardiac	SPECT/CT and PET/CT	-	1.60	2.20	35.00	53.00
Dennis ³¹	2018	CT cardiac	SPECT/CT	AC	-	1.85	-	39.00
Lima ³⁰	2018	CT cardiac	SPECT/CT and PET/CT	AC/AL	1.00	2.00	10.00	40.00
Iball ³³	2017	CT cardiac	SPECT/CT	AC	1.60	2.10	34.00	36.00

Table 10. Comparison of CT in MPI against other published MPI studies in terms of CTDI_{vol} and DLP. AC – Attenuation correction, AL – Anatomical localization, Dx – Diagnostic.

ED	MPI protocol	Effective dose (mSv)				p-value
		Mean \pm SD	Median	Min	Max	
ED _{SPECT}	One-day	5.42 \pm 1.33	5.16	3.32	11.72	
	Two-day	11.10 \pm 3.96	12.66	2.07	17.17	
ED _{CT}	CTAC One-day	1.42 \pm 0.78	1.32	0.57	4.53	
	CTAC Two-day	2.26 \pm 0.87	2.46	0.74	3.65	
ED _{CUMULATED}	CAC One-day	1.87 \pm 0.27	1.76	1.01	3.30	<0.001 ^a
	CAC Two-day	1.94 \pm 0.31	1.76	1.51	2.93	
ED _{CUMULATED}	One-day/CTAC	6.69 \pm 1.76	6.50	4.10	11.36	<0.001 ^a
	One-day/CAC	7.32 \pm 1.37	7.04	5.20	13.48	
	Two-day/CTAC	10.13 \pm 5.31	6.87	2.81	16.62	0.001 ^a
	Two-day/CAC	13.99 \pm 3.24	14.53	5.86	19.20	

Table 11. Distribution of cumulated effective dose for across MPI protocols. a – Independent t-test.

Next, both the mean CTDI_{vol} and DLP values in the CAC protocol are higher values compared to CTAC. This is because the CAC protocol utilizes CT axial acquisition, gated scan mode with fixed scan parameters resulting in higher tube current and voltage, which generally leads to higher radiation dose. The CAC protocol is a favorable element in clinical practice as it provides valuable information associated to perfusion findings, including tissue characterization and calcium score determination in the coronary arteries^{11,12}. Furthermore, the DRL and AD values of CTDI_{vol} in CAC protocol are comparable due to the fixed nature of the protocol parameters, which allow for nearly consistent CTDI_{vol} normalisation using a 32 cm body phantom, despite variations in the subjects' actual body proportions. Although not analyzed in the study, the size-specific dose estimate (SSDE) method, as proposed by the American Association of Physicists in Medicine (AAPM) Report 204, may serve as an alternative approach to determine actual CTDI_{vol}. The SSDE calculation is based on conversion factors estimated from the subjects' actual body size offering a more individualized dose assessment.

Comparison with other similar findings

SPECT

There are several possible causes for variations in DRL and AD for MPI studies in our data compared to the others. First, the variations of body habitus and weight across regions can impact radiation doses. Heavier patients may require higher doses to obtain acceptable image quality²². Apart from that, variations in equipment might also play a role. It has been widely reported that CZT based technology is superior to conventional SPECT system^{35,36}. With CZT, a low radiation dose is required to produce adequate image quality. When compared to a center without CZT based technology, a center with it may report lower DRL and AD values. Regional practice patterns may also have an impact, as seen by the distinctly varied practices observed across different global locations, which suggests, a lack of standardization in MPI practice²⁴. Nonetheless, several well recognized guidelines could serve as foundation for practice adaptation before being modified to suit local preferences^{17,37}. In short, differences in patient body habitus, imaging protocols, equipment, and regional practice patterns all likely contribute to the variations seen in MPI DRLs worldwide. Standardizing practices globally could help optimize radiation doses for these common nuclear cardiology procedures.

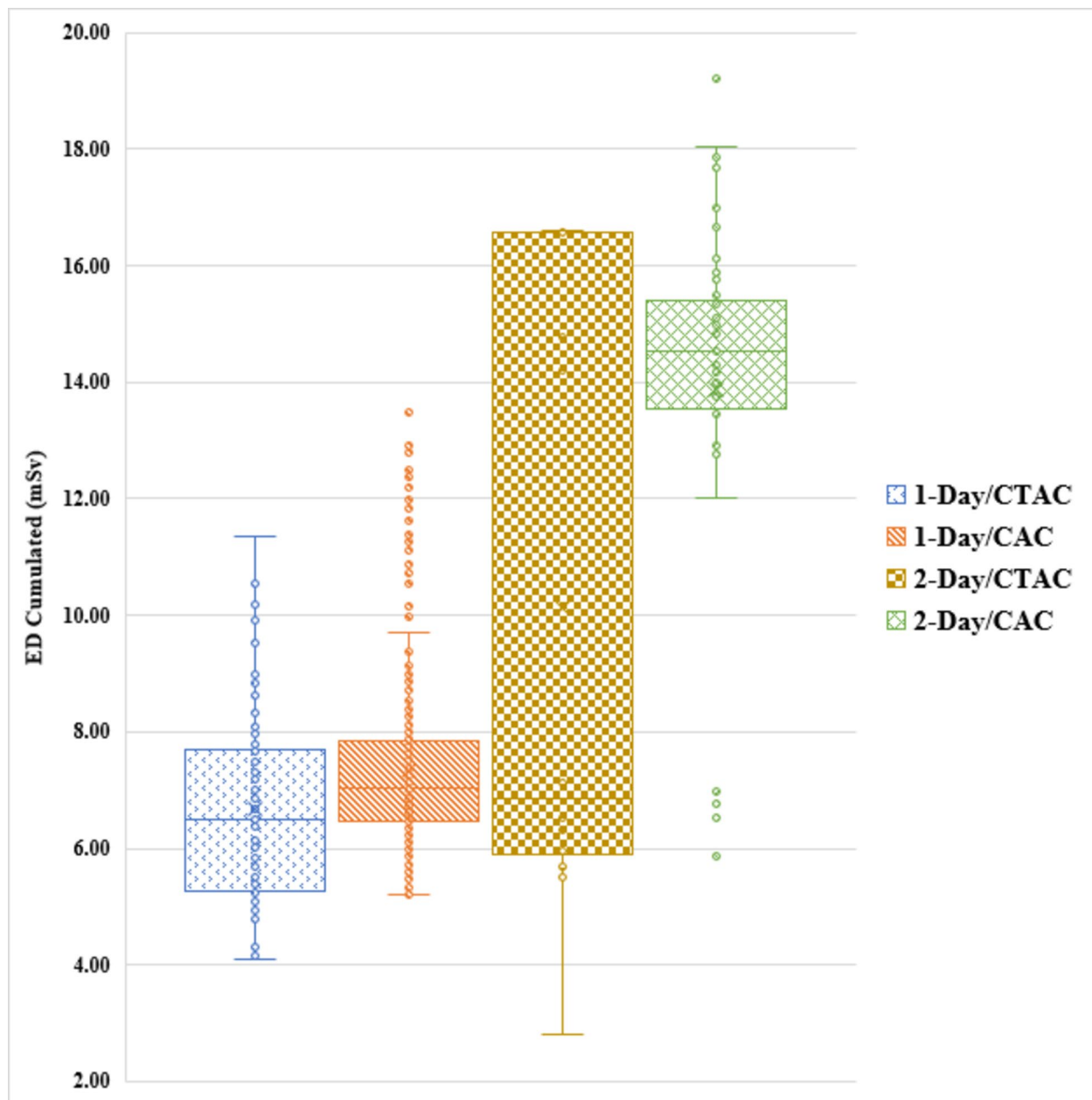


Fig. 1. Distribution of cumulated effective dose for across MPI protocols.

Protocol	Relative contribution (%)	
	SPECT	CT
One-day/CTAC	79.5%	20.5%
One-day/CAC	73.8%	26.2%
Two-day/CTAC	74.9%	25.1%
Two-day/CAC	85.0%	15.0%
Average contribution	78.3%	21.7%

Table 12. Relative contribution of SPECT and CT in MPI protocol.

CT

The main factors contributing to variations in CT doses in MPI studies compared to other similar studies can stem from several factors such as local parameters technical preferences, scanner technology differences, scan indications, radiographer practices and patient characteristics^{38,39}. Therefore, standardizing scanning protocols and educate the operators on the importance of consistent scan lengths are crucial steps to minimize dose variations. Understanding these contributing factors can help in optimizing protocols and reducing unnecessary radiation exposure to patients, ultimately improving the quality and safety of MPI studies.

Effective dose (ED)

American Society of Nuclear Cardiology (ASNC) has stated that ED of 9 mSv or below is considered as the best MPI study practice. In our data, radiation doses of < 9 mSv were achieved in the one-day protocol but not in the two-day protocol. Based on this finding, there is a need for reduction of radiation exposure in the practice. Identifying on which modality carries the highest radiation burden is crucial, as this information can guide the development of a radiation dose optimization strategy. The result of this study showed that SPECT contributes a higher radiation dose than CT. Consequently, optimization efforts for SPECT should begin with a review of the activity prescription protocol, with particular attention to the two-day protocol. Given that most patients undergoing the two-day protocol are assigned to GC-2, optimization should focus on refining practices associated with GC-2. There are several ways to reduce radiation exposure in GC-2 protocol. Firstly, to be more proactive in performing stress-only imaging procedure. Alertness to the normal stress images is needed to avoid the subsequent rest imaging, whenever applicable. By doing this, up to 80% of radiation dose reduction could be achieved^{24,40,41}.

Furthermore, a camera-based reduction strategy could also help to reduce radiation dose. This includes incorporating alternative settings in iterative reconstruction, resolution recovery, and noise modulation, that cope with lower cardiac SPECT counting statistics and thereby provide acceptable image quality despite reduced SPECT acquisition time and/or reduced injected radiopharmaceutical activity. By doing this, activity prescriptions could be set lower, even for heavier patient^{42–44}. However, any changes to image reconstruction parameters should be made in close collaboration with the reporting clinician to ensure that the adjustments do not significantly alter the image quality from the perspective of the image interpreter. Another recommendation is to consider for positron emission tomography (PET) MPI, as it could help to reduce radiation dose. However, its feasibility may be limited due to the high cost of the procedure and the availability of PET radiopharmaceuticals^{41,45,46}.

This study has several limitations. Since the study was conducted at a single tertiary cardiac center, the results may not be fully representative of other institutions with different imaging equipment, protocols, or patient demographics. Future studies should adopt a multi-centre approach involving diverse institutions with varying imaging protocols, equipment types, and patient demographics. This would enhance the robustness of the data, ensuring the established DRLs and ADs are more representative of national or regional practices. Next, as the study only included adult subjects, the established DRLs and ADs may not apply to younger populations requiring distinct imaging protocols. Future research should focus on conducting a separate study specifically targeting paediatric and younger adult populations to establish appropriate DRLs and ADs for these groups.

Lastly, while this study proposed optimization strategies, no active intervention was conducted to assess their clinical impact. Future efforts should focus on implementing these strategies and evaluating their effectiveness in clinical practice. This is particularly important given the higher ED observed in patients scanned using GC-2, emphasizing the need for targeted interventions to reduce radiation exposure while maintaining diagnostic accuracy. Recognizing this, we have acknowledged it as a study limitation to highlight the need for future research exploring active intervention strategies for dose optimization and their potential impact on the generalizability of the established DRLs.

Conclusion

Local DRL and AD data for MPI procedures have been successfully established, along with the calculation of ED from the MPI study to assess the variations in radiation doses received from each component. These data serve as supplementary information to support professional judgments that weigh the benefits and risks of ionizing radiation in medical imaging, rather than as a constraint on the appropriate use of medical radiation. To ensure patient safety, applying the as low as reasonably achievable (ALARA) principle consistently in medical radiation practices is needed. Consequently, this ensures that patient safety remains a top priority while still achieving adequate diagnostic outcomes. Establishing local DRLs and the calculation of ED are valuable tools for guiding radiological practices, but they should complement, not replace, clinical judgment. By adhering to the ALARA principle, healthcare professionals can effectively balance the need for diagnostic accuracy with the imperative to minimize radiation exposure, ultimately contributing to safer and more effective medical imaging practices.

Data availability

The datasets used and/or analysed during the current study available from the corresponding author on reasonable request.

Received: 15 December 2024; Accepted: 1 April 2025

Published online: 11 April 2025

References

1. Bicknell, K. A. & Brooks, G. Reprogramming the cell cycle machinery to treat cardiovascular disease. *Curr. Opin. Pharmacol.* **8**(2), 193–201. <https://doi.org/10.1016/J.COPH.2007.12.015> (2008).

2. Brown, J. C., Gerhardt, T. E. & Kwon, E. Risk factors for coronary artery disease. [Updated 2022 Jun 5]. In *StatPearls [Internet] Treasure Island (FL): StatPearls Publishing*; 2022. Published online 2022.
3. Hosny, T., Khalil, M. M., Elfify, A. A. & Elshemey, W. M. Image quality characteristics of myocardial perfusion SPECT imaging using state-of-the-art commercial software algorithms: Evaluation of 10 reconstruction methods. *Am. J. Nucl. Med. Mol. Imaging* **10**(6), 375–386 (2020).
4. Ora, M. & Gambhir, S. Myocardial perfusion imaging: A brief review of nuclear and nonnuclear techniques and comparative evaluation of recent advances. *Indian J. Nucl. Med.* **34**(4), 263–270. https://doi.org/10.4103/ijnm.IJNM_90_19 (2019).
5. Galassi, A. R., Azzarelli, S. & Tomaselli, A. et al. Incremental prognostic value of technetium-99m-tetrofosmin exercise myocardial perfusion imaging for predicting outcomes in patients with suspected or known coronary artery disease. Published online 2001.
6. Gimelli, A. et al. Stress/rest myocardial perfusion abnormalities by gated SPECT: Still the best predictor of cardiac events in stable ischemic heart disease. *J. Nucl. Med.* **50**(4), 546–553. <https://doi.org/10.2967/jnumed.108.055954> (2009).
7. Herzog, B. A. et al. Nuclear myocardial perfusion imaging with a cadmium-zinc-telluride detector technique: Optimized protocol for scan time reduction. *J. Nucl. Med.* **51**(1), 46–51. <https://doi.org/10.2967/jnumed.109.065532> (2010).
8. Mettler, F. A. & Guiberteau, M. J. Cardiovascular System. In *Essentials of Nuclear Medicine and Molecular Imaging* 7th edn (eds Mettler, F. A. & Guiberteau, M. J.) 116–174 (Elsevier, 2019). <https://doi.org/10.1016/B978-0-323-48319-3.00005-5>.
9. Ziessman, H. A., O'Malley, J. P. & Thrall, J. H. In the requisites in radiology. In *Nuclear Medicine* 263–301 (Mosby, 2006). <https://doi.org/10.1016/B978-0-323-02946-9.50014-3>.
10. Patel, J. J. & Alzahrani, T. Myocardial perfusion scan. StatPearls, January 2021. Accessed 24 Dec 2023. <https://www.ncbi.nlm.nih.gov/books/NBK539772/>
11. Yokota, S. et al. Coronary calcium score influences referral for invasive coronary angiography after normal myocardial perfusion SPECT. *J. Nucl. Cardiol.* **26**(2), 602–612. <https://doi.org/10.1007/s12350-017-1067-9> (2019).
12. Sharma, V. et al. The additive prognostic value of coronary calcium score (CCS) to single photon emission computed tomography myocardial perfusion imaging (SPECT-MPI)-real world data from a single center. *J. Nucl. Cardiol.* **28**(5), 2086–2096. <https://doi.org/10.1007/s12350-019-01965-9> (2021).
13. Schenker, M. P. et al. Interrelation of coronary calcification, myocardial ischemia, and outcomes in patients with intermediate likelihood of coronary artery disease: A combined positron emission tomography/computed tomography study. *Circulation* **117**(13), 1693–1700. <https://doi.org/10.1161/CIRCULATIONAHA.107.717512> (2008).
14. Becker, M. D. et al. U.S. PET/CT and gamma camera diagnostic reference levels and achievable administered activities for noncardiac nuclear medicine studies. *Radiology* **293**(1), 203–211. <https://doi.org/10.1148/radiol.2019190623> (2019).
15. ICRP. *ICRP Publication 135: Diagnostic Reference Levels in Medical Imaging*. 2017. Accessed 10 Dec 2023. <https://www.icrp.org/publication.asp?fid=ICRP%20Publication%20135>
16. Banks, K. P. et al. Diagnostic reference levels and achievable administered activities for adult renal scintigraphy: An analysis of the intersocietal accreditation committee nuclear laboratories. *J. Nucl. Med. Technol.* **49**(3), 246–249. <https://doi.org/10.2967/jnmt.120.261552> (2021).
17. Henzlova, M. J., Duvall, W. L., Einstein, A. J., Travin, M. I. & Verberne, H. J. ASNC imaging guidelines for SPECT nuclear cardiology procedures: Stress, protocols, and tracers. *J. Nucl. Cardiol.* **23**(3), 606–639. <https://doi.org/10.1007/s12350-015-0387-x> (2016).
18. Fiechter, M. et al. Cadmium-zinc-telluride myocardial perfusion imaging in obese patients. *J. Nucl. Med.* **53**(9), 1401–1406. <https://doi.org/10.2967/jnmed.111.102434> (2012).
19. Andersson, M. Erratum to: Effective dose to adult patients from 338 radiopharmaceuticals estimated using ICRP biokinetic data, ICRP/ICRU computational reference phantoms and ICRP 2007 tissue weighting factors(EJNMMI Physics). *EJNMMI Phys.* **2**(1), 1–7. <https://doi.org/10.1186/s40658-015-0121-4> (2015).
20. Andersson, M., Johansson, L., Minarik, D., Leide-Svengborn, S. & Mattsson, S. Effective dose to adult patients from 338 radiopharmaceuticals estimated using ICRP biokinetic data, ICRP/ICRU computational reference phantoms and ICRP 2007 tissue weighting factors. 2014. <https://doi.org/10.1186/2197-7364-1-9>
21. Trattner, S. et al. Cardiac-specific conversion factors to estimate radiation effective dose from dose-length product in computed tomography. *JACC Cardiovasc. Imaging* **11**(1), 64–74. <https://doi.org/10.1016/j.jcmg.2017.06.006> (2018).
22. Alkhybari, E. et al. Radiation dose assessment for myocardial perfusion imaging: A single institution survey. *Tomography* **9**(1), 264–273. <https://doi.org/10.3390/tomography9010021> (2023).
23. Australian Radiation Protection and Nuclear Safety Agency (ARPANSA). *Australian National Diagnostic Reference Levels for Nuclear Medicine Australian Diagnostic Reference Levels for Nuclear Medicine*. 2023. www.arpansa.gov.au/ndrls
24. Hirschfeld, C. B. et al. Worldwide diagnostic reference levels for single-photon emission computed tomography myocardial perfusion imaging: Findings from INCAPS. *JACC Cardiovasc. Imaging* **14**(3), 657–665. <https://doi.org/10.1016/j.jcmg.2020.06.029> (2021).
25. Abe, K. et al. The 2020 national diagnostic reference levels for nuclear medicine in Japan. *Ann. Nucl. Med.* **34**(11), 799–806. <https://doi.org/10.1007/s12149-020-01512-4> (2020).
26. Song, H. C. et al. Diagnostic reference levels for adult nuclear medicine imaging established from the National Survey in Korea. *Nucl. Med. Mol. Imaging* **53**(1), 64–70. <https://doi.org/10.1007/s13139-019-00585-y> (2019).
27. Willegaigron, J. et al. Diagnostic reference level: An important tool for reducing radiation doses in adult and pediatric nuclear medicine procedures in Brazil. *Nucl. Med. Commun.* **37**(5), 525–533. <https://doi.org/10.1097/MNM.0000000000000462> (2016).
28. Ministry of Health Malaysia. Guidelines on diagnostic reference level in nuclear medicine. 2013.
29. Rinscheid, A. et al. Radiation doses from low-dose CT scans in SPECT/CT and PET/CT examinations: A survey in Germany. *Nuklearmedizin-NuclearMedicine* **61**(04), 294–300 (2022).
30. Bebbington, N. A. et al. A Nordic survey of CT doses in hybrid PET/CT and SPECT/CT examinations. *EJNMMI Phys.* <https://doi.org/10.1186/s40658-019-0266-7> (2019).
31. Dennis, J. L., Gemmell, A. J. & Nicol, A. J. Optimization of the CT component of SPECT-CT and establishment of local CT diagnostic reference levels for clinical practice. *Nucl. Med. Commun.* **39**(6), 493–499. <https://doi.org/10.1097/MNM.0000000000000831> (2018).
32. Lima, T. V. M. et al. Swiss survey on hybrid imaging CTs doses in nuclear medicine and proposed national dose reference levels. *Z Med. Phys.* **28**(4), 265–275. <https://doi.org/10.1016/j.zemedi.2018.01.005> (2018).
33. Iball, G. R. et al. A national survey of computed tomography doses in hybrid PET-CT and SPECT-CT examinations in the UK. *Nucl. Med. Commun.* **38**(6), 459–470 (2017).
34. Kao, Y. H. & Better, N. D-SPECT: New technology, old tricks. *J. Nucl. Cardiol.* **23**(2), 311–312. <https://doi.org/10.1007/s12350-015-0290-5> (2016).
35. Duvall, W. L. et al. Comparison of high efficiency CZT SPECT MPI to coronary angiography. *J. Nucl. Cardiol.* **18**(4), 595–604. <https://doi.org/10.1007/s12350-011-9382-z> (2011).
36. Wells, R. G. et al. Reduction of injected activity for MBF with a CZT Cardiac SPECT Camera. *J. Nucl. Med.* **65**(supplement 2), 242197 (2024).
37. Verberne, H. J. et al. EANM procedural guidelines for radionuclide myocardial perfusion imaging with SPECT and SPECT/CT: 2015 revision. *Eur. J. Nucl. Med. Mol. Imaging* **42**(12), 1929–1940. <https://doi.org/10.1007/s00259-015-3139-x> (2015).
38. Damilakis, J. et al. How to establish and use local diagnostic reference levels: an ESR EuroSafe Imaging expert statement. *Insights Imaging* <https://doi.org/10.1186/s13244-023-01369-x> (2023).

39. Paulo, G. et al. Diagnostic reference levels based on clinical indications in computed tomography: A literature review. *Insights Imaging* **11**(1), 96. <https://doi.org/10.1186/s13244-020-00899-y> (2020).
40. Partington, S. L. et al. Reducing radiation dose from myocardial perfusion imaging in subjects with complex congenital heart disease. *J. Nucl. Cardiol.* **28**(4), 1395–1408. <https://doi.org/10.1007/s12350-019-01811-y> (2021).
41. Gimelli, A. et al. Strategies for radiation dose reduction in nuclear cardiology and cardiac computed tomography imaging: A report from the European Association of Cardiovascular Imaging (EACVI), the Cardiovascular Committee of European Association of Nuclear Medicine (EANM), and the European Society of Cardiovascular Radiology (ESCR). *Eur. Heart J.* **39**(4), 286–296. <https://doi.org/10.1093/eurheartj/ehx582> (2018).
42. Wells, R. G., Renaud, J., DeKemp, R. & Ruddy, T. Dose reduction for SPECT MBF measurement with a dedicated cardiac camera. *J. Nucl. Med.* **58**(supplement 1), 229 (2017).
43. Kim, D. A., Farrell, M. B. & Jerome, S. D. It's about time we think about lowering radiation dose in obese patients too. *J. Nucl. Cardiol.* **24**(6), 1922–1925. <https://doi.org/10.1007/s12350-016-0636-7> (2017).
44. Papanastasiou, E., Theodoridou, E., Doumas, A., Gerasimou, G. & Siountas, A. A study on the optimization of the administered activity in myocardial perfusion SPECT imaging with Tc-99m according to body measurements. *Phys. Med.* **68**, 69–74. <https://doi.org/10.1016/j.ejmp.2019.11.011> (2019).
45. Dobrala, S. et al. Approaches to reducing radiation dose from radionuclide myocardial perfusion imaging. *J. Nucl. Med.* **56**(4), 592–599. <https://doi.org/10.2967/jnumed.112.115097> (2015).
46. Prasad, K., Adams, C., Quang, E. & Stocker, D. The effect of BMI on high versus low administered activity protocol MPI scan time using a CZT camera in clinical practice. *J. Nucl. Med.* **62**(supplement 1), 1643 (2021).

Acknowledgements

We would like to express our deepest gratitude to the IJN Foundation for funding the publication of this study, to the Clinical Research Department for their invaluable guidance throughout the completion of this research, and to the Imaging Centre for their unwavering moral support.

Author contributions

All authors contributed to the study conception and design. Material preparation, data collection and analysis were performed by Haniff Shazwan Muhammad Safwan Selvam, Norizan Omar, Azuan Nazri and Ali Hazizi Jamal Harizan. The first draft of the manuscript was written by Haniff Shazwan Muhammad Safwan Selvam and all authors commented on previous versions of the manuscript. All authors read, improvised and approved the final manuscript.

Declarations

Competing interests

The authors declare no competing interests.

Ethical approval

The study received full approval from the IJN Research Ethics Committee (IJNREC/651/2024), with a waiver for informed consent granted prior to its initiation. Data collection has been carried out in accordance to relevant guideline and regulations.

Additional information

Correspondence and requests for materials should be addressed to H.S.S.S.

Reprints and permissions information is available at www.nature.com/reprints.

Publisher's note Springer Nature remains neutral with regard to jurisdictional claims in published maps and institutional affiliations.

Open Access This article is licensed under a Creative Commons Attribution-NonCommercial-NoDerivatives 4.0 International License, which permits any non-commercial use, sharing, distribution and reproduction in any medium or format, as long as you give appropriate credit to the original author(s) and the source, provide a link to the Creative Commons licence, and indicate if you modified the licensed material. You do not have permission under this licence to share adapted material derived from this article or parts of it. The images or other third party material in this article are included in the article's Creative Commons licence, unless indicated otherwise in a credit line to the material. If material is not included in the article's Creative Commons licence and your intended use is not permitted by statutory regulation or exceeds the permitted use, you will need to obtain permission directly from the copyright holder. To view a copy of this licence, visit <http://creativecommons.org/licenses/by-nc-nd/4.0/>.

© The Author(s) 2025